JOURNAL OF GEOPHYSICAL RESEARCH, VOL. 108, NO. D20, 8783, doi:10.1029/2002JD003108, 2003

Air motion intercomparison flights during Transport and Chemical Evolution in the Pacific (TRACE-P)/ACE-ASIA

K. Lee Thornhill
Science Applications International Corporation (SAIC)

Bruce E. Anderson, John D. W. Barrick, and Donald R. Bagwell
NASA Langley Research Center, Hampton, Virginia, USA

Richard Friesen and Donald H. Lenschow
National Center for Atmospheric Research, Boulder, Colorado, USA

Received 31 October 2002; revised 8 April 2003; accepted 1 May 2003; published 30 September 2003.

[1] Intercomparisons of chemical, aerosol, and meteorological measurement systems were conducted in the spring of 2001 between the NASA Wallops P3-B and the NCAR EC-130Q aircraft during overlapping portions of the concurrent tropospheric missions: the Global Tropospheric Experiment's (GTE) Transport and Chemical Evolution in the Pacific (TRACE-P) and Aerosol Characterization Experiment's ACE-ASIA mission, respectively. Both aircraft were equipped with similar air-motion measurement systems and in situ meteorology sensors designed to measure the eddy-correlation fluxes of momentum, heat, and water vapor. This paper presents the results of the informal intercomparison flight legs at two altitudes within the marine boundary layer performed over the Sea of Japan. The variances and spectra of the three-dimensional winds and temperature are presented along with the cospectra of the vertical velocities and various parameters. The results show good agreement between the measurements obtained from the two aircraft. Discrepancies in the data are analyzed and discussed. *INDEX TERMS:* 3307 Meteorology and Atmospheric Dynamics: Boundary layer processes; 3379 Meteorology and Atmospheric Dynamics: Turbulence; 3394 Meteorology and Atmospheric Dynamics: Instruments and techniques; 3399 Meteorology and Atmospheric Dynamics: General or miscellaneous; *KEYWORDS:* turbulence, aircraft, flux, intercomparison

Citation: Thornhill, K. L., B. E. Anderson, J. D. W. Barrick, D. R. Bagwell, R. Friesen, and D. H. Lenschow, Air motion intercomparison flights during Transport and Chemical Evolution in the Pacific (TRACE-P)/ACE-ASIA, *J. Geophys. Res.*, *108*(D20), 9001, doi:10.1029/2002JD003108, 2003.

1. Introduction

[2] Aircraft provide an excellent research platform for characterization of the atmospheric boundary layer [*Lenschow*, 1986]. Aircraft mobility enables a large area to be sampled in a short period of time. Airborne measurements are an important link between atmospheric data sets obtained from stationary ground sites and remote satellites. Advances in airborne in situ instrumentation and avionics have significantly improved the accuracy of air motion measurements such as winds, temperature, and humidity. The ability to make fast response measurements and cover a large range of frequencies allows turbulence fluxes of heat, momentum, and chemical species to be measured. These measurements are complex owing to the need for high precision and fast response sensors to measure the air velocity and aircraft motions. The distortion of the airflow around an aircraft is unique due to fuselage shape and sensor location and makes ground calibrations of the air motion sensors infeasible. As a result, in-flight calibrations are required.

[3] One way to objectively check the performance of an air motion system is to compare the measurements between aircraft while both planes are flying in close formation [*Lenschow et al.*, 1991; *MacPherson et al.*, 1992]. An intercomparison can help point out possible problems in calibration techniques or sensor measurements and give additional confidence to air motion measurements.

[4] In the spring of 2001 a unique opportunity arose for two aircraft to intercompare the performance of their respective air motion systems over the Sea of Japan. The NASA P-3B Orion (hereafter referred to as the P3B) aircraft was deployed on the NASA Transport and Chemical Evolution in the Pacific (TRACE-P) mission to characterize the outflow of emissions from the Asian continent. TRACE-P was the latest in the series of aircraft-based field missions undertaken by NASA's Global Tropospheric Experiment (GTE) [*Jacob et al.*, 2003]. Concurrently, the National Center for Atmospheric Research (NCAR) EC-130Q Hercules (hereafter referred to as the C130) was deployed in the same area for the Aerosol Characterization Experiment

0148-0227/03/2002JD003108

Table 1. Atmospheric Sensors Used in the TRACE-P/ACE-ASIA Air Motion Intercomparison

Parameter	NASA P-3B	NCAR EC-130Q
Airspeed Vector	Radome ports	Radome ports
Earth-referenced velocity vector	Litton LTN-72RH Inertial Navigation System	Honeywell LaserRef SM Inertial Reference System
Temperature—Fast response	Rosemount Model 102E4AL	Rosemount Model 102E2AL
Water vapor—Slow response	General Eastern 1011B	General Eastern 1011B
Water vapor—Fast response	Lyman-Alpha Hygrometer Model AIR-LA-1AC	Lyman-Alpha Hygrometer Model NCAR Developed LA-3
Sampling Rate	50 s^{-1}	$\geq$25 s^{-1}

(ACE-ASIA) (details available at http://saga.pmel.noaa.gov/aceasia/). This was the fourth in a series of International Global Atmospheric Chemistry (IGAC) field experiments. It was designed to increase the understanding of the effects of atmospheric aerosols on the Earth's climate.

[5] The spatial and temporal overlap in the field missions provided the two instrument intercomparison opportunities. The P3B was based at Yokota Air Force Base in Fussa, Japan, while the ACE-ASIA mission operated out of Iwakuni Marine Corps Air Station Base in Iwakuni, Japan. Closely coordinated flight legs were flown on 30 March and 2 April 2001 over the Sea of Japan to compare the chemical and aerosol sensors on the two aircraft. The flight plan included constant altitude runs in the marine boundary layer (MBL) and lower-free troposphere, ramp ascents/descents, and spiral ascents/descents. Even though the primary goal of these flight maneuvers was not to intercompare the air-motion systems, the multiple legs in the MBL lasting anywhere from 10 to 60 min provided an opportunity for comparing the means, variances, and fluxes obtained from the two systems.

[6] This paper focuses upon results obtained during the second intercomparison flight on 2 April 2001. The results of the intercomparison flight legs, including the means, variances, and covariances (fluxes), are presented and analyzed. An examination of the means, variances, and covariances provides a basis for evaluating the relative agreement between the two systems and determining whether discrepancies may be due to instrument problems or simply the result of aircraft separation coupled with spatial inhomogeneities in the ambient meteorological fields.

2. Aircraft and Instrumentation

[7] Both the P3B and the C130 have been equipped with instrumentation to measure the three-dimensional winds along with fast response measurements of water vapor and temperature. In addition, they are able to accept inputs of fast response chemical species sensors such as CO_2, O_3, and SO_2. From these inputs, eddy correlation fluxes can be computed. An air-motion system such as the ones installed on the NASA and NCAR aircraft are essentially composed of three parts: (1) a radome flush port differential pressure system, (2) an inertial navigation system (INS) to measure the aircraft's position, speed, and attitude relative to the Earth, and (3) a data acquisition system to record all the incoming signals.

[8] A radome differential pressure system determines the angles of the ambient airflow relative to the aircraft from pressure fluctuations on the nose of the aircraft [*Brown et al.*, 1983; *Larson et al.*, 1980]. Five flush ports are installed in a cruciform pattern in the nose of the aircraft that allow for measurement of the angle of attack (vertically stacked holes) and the sideslip angle (horizontally aligned holes). In addition, the center hole, positioned on the stagnation point of the radome, can be linked to the existing static pressure port of the aircraft to obtain the impact (dynamic) and total pressure measurements. A summary of the on-board air motion sensors on the two aircraft is provided in Table 1.

[9] Three-dimensional winds are computed from the full air motion equations [*Lenschow*, 1986]. The vertical platform velocity components are computed from a third-order baro-loop, which limits the errors in vertical acceleration by bounding the doubly integrated vertical acceleration by the pressure altitude [*Blanchard*, 1971; *Lenschow*, 1986]. The NCAR and NASA algorithms are very similar, with the only differences being the time constants used in the baro-loop computation.

2.1. NASA P3-B Orion Turbulent Air Motion Measurement System (TAMMS)

[10] The Wallops P3-B Orion is a four-engine turboprop plane utilized during GTE Tropospheric missions for low-altitude boundary layer studies. The flight ceiling for the P3B is 9.1 km; however the highest altitude obtained during TRACE-P was about 7.6 km. The typical science flight for the TRACE-P mission lasted 8–10 hours. The nominal true airspeed of the P3-B is 100 m s^{-1}. The GTE project office at NASA Langley Research Center, Hampton, Virginia supports the air motion system on the NASA P3-B.

[11] In addition to the radome differential pressure system, the TAMMS utilizes Rosemount 858Y hemispherical flow-direction probes as backups. One is placed on the side of the fuselage for angle of attack measurements, while the other, placed on the top of the fuselage, serves to measure the sideslip angle of the ambient airflow. Pressure transducers are placed as close as possible to the pressure ports in order to minimize delays and errors [*Considine et al.*, 1999]. The Rosemount 858Y sensors are positioned alongside the cockpit of the P3B and the time lag from this displacement is well characterized and accounted for in the data processing. One of the unpublished results of this analysis was comparing the results obtained by the radome and the 858Y probes. All calculated winds, variances, and covariances for the P3B could be reproduced by both the radome and 858Y systems.

[12] Ambient air temperature is measured on the P3B by a Rosemount Model 102 non-deiced total air temperature sensors using fast response platinum sensing elements (E102E4AL) [*Deleo and Werner*, 1960]. Redundant sensors are located on either side of the radome. Contamination from sea-salt spray has occurred in the past due to low-altitude flux flights over the ocean that can create an electrical short across the sensing element windings [*Considine et al.*, 1999; *Schmitt et al.*, 1978].

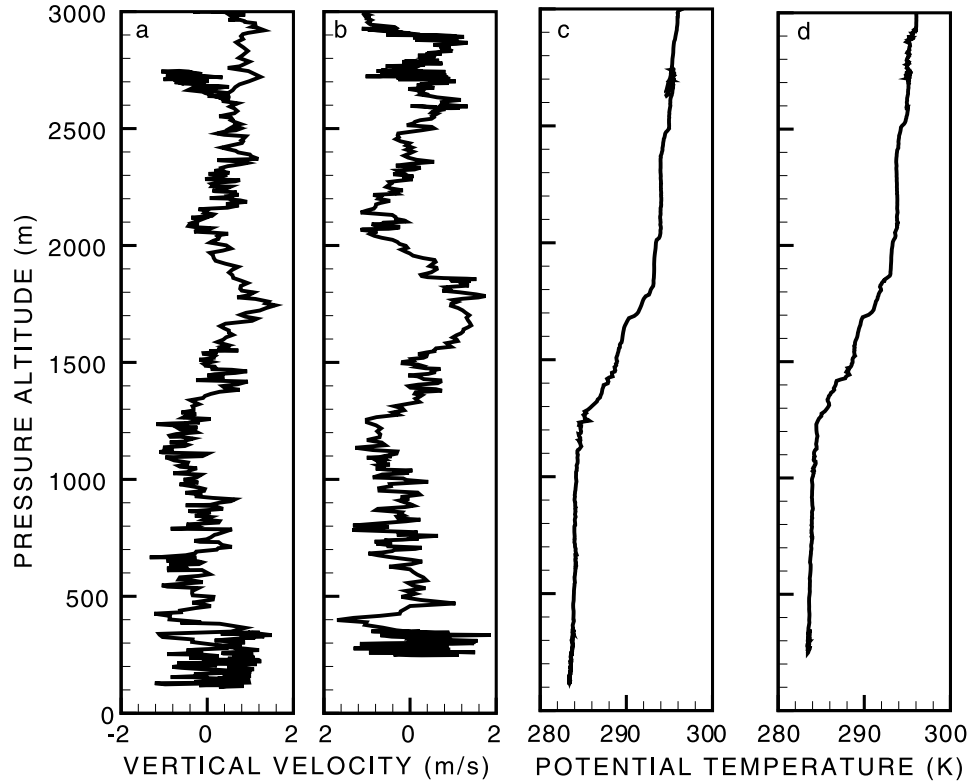

Figure 1. Vertical soundings for P3B Flight 19 (spiral descent at 0155:40 UTC) of (a–b) vertical wind velocity and (c–d) potential temperature (K) for the NCAR C130 (Figures 1a and 1c) and the NASA P3B (Figures 1b and 1d). The top of the mixed layer is about 1.2 km.

[13] Fast response water vapor is measured by a Lyman-Alpha hygrometer (model AIR-LA-1AC). Since this instrument is not an absolute humidity sensor, the fast response output of the Lyman-Alpha is calibrated via a post-processing algorithm to a slow response absolute humidity source, the General Eastern 1011B hygrometer. The combination of the two hygrometers provides high-precision fast response humidity measurements without the drift inherent in the Lyman-Alpha signal. Unfortunately, the TAMMS Lyman-Alpha source was nearing extinction by the time of the intercomparison period and was not operating during the second formation flight.

[14] The aircraft motion and position measurements were acquired from a Litton Model LTN-72RH inertial navigation system (INS). The INS has a drift rate of approximately 0.4 km/h (C. Robinson, Litton Industries, personal communication, 1998). Unfortunately, the P3B is not equipped with the ability to use Global Positioning Satellite (GPS) data to correct the INS for long-term drift.

2.2. NCAR EC-130Q Hercules

[15] The Lockheed EC-130Q Hercules is a four-engine turboprop aircraft, with a maximum ceiling of 7.9 km and an endurance of about 10 hours, while operating at a typical true air speed of 100 m s^{-1}. Like the NASA P3B, the aircraft was instrumented for a variety of chemical and aerosol species, in addition to the air motion sensing system.

[16] The fast response temperature on the C130 is measured by two Rosemount sensors, a non-deiced version (Model 102E2AL), and a deiced version (Model 102E). In addition, an infrared thermometer by Ophir Corporation is used to determine the ambient air temperature. The C130 measures humidity in the same way as the P3B, with a fast-response Lyman-Alpha hygrometer (NCAR Developed LA-3 hygrometer) tied to a slower-response General Eastern Instrument's 1011B hygrometer. The post processing algorithms used by the two groups (NASA and NCAR) are essentially the same, with the only differences being in the coefficients used.

[17] The aircraft position for the C130 is determined from a Honeywell LaserRef SM Inertial Reference System. The drift in the INS is corrected via GPS measurements from the Trimble Navigation Model TANS III system. It has been shown that correcting for the drift inherent in INS systems can account for both the Schuler oscillation (about ± 1 m s^{-1}) and higher-frequency oscillations (about ± 0.5 ms^{-1}) [*Khelif et al.*, 1999].

3. Methodology

[18] This was the first time that either the P3B or the C130 had the opportunity to compare air motion systems with other aircraft in conditions suitable for measuring eddy correlation fluxes of meteorological components. However, both aircraft have participated in multiple flight campaigns where air motion measurements were made and used by the science community. The NCAR aircraft have a long history of air motion measurements and intercomparisons [*Lenschow and Spyers-Duran*, 1989; *Lenschow*, 1986; *Lemone and Pennell*, 1981; *Dobosy et al.*, 1997; *Lenschow et al.*, 1991;

Table 2. Details of the Intercomparison Runs From P3-B Flight 19 on 2 April 2001 (Boundary Layer Height = 1.2 km)

Time, GMT	Altitude, m	Length of Leg, km	Heading, deg	Wind Direction, deg
0216–0226	152	57.8	41	227
0233–0302	152	171	180	210
0314–0340	610	151.6	344	227

MacPherson et al., 1992]. The NASA P3B TAMMS and its predecessor aboard the NASA Electra have been used in multiple field campaigns funded by NASA's GTE Program [*Considine et al.*, 1999; *Ritter et al.*, 1992; *Ritter et al.*, 1994; *Ritter et al.*, 1990; *Barrick et al.*, 1996] but never intercompared with similar aircraft.

[19] On 30 March and 2 April 2001, intercomparison flights were performed over the Sea of Japan. The planes flew wing-to-wing for a total of 5.5 hours over the course of the two flights, making measurements at several altitudes, both in the MBL and in the free troposphere. During the first intercomparison flight (30 March) the C130 science team planned the altitudes and durations of the flight legs. During the second intercomparison flight (2 April), the P3B flew as the lead aircraft with the C130 flying in the role of the trailing aircraft at the nominal true air speed of 100 m s^{-1}.

[20] The second intercomparison flight on 2 April (Flight 19 for the P3B and RF02 for the C130) took place over the Sea of Japan, along an axis of low-level outflow, with the flight legs stacked in a wall pattern to intercept the continental outflow. There were scattered cumulus clouds, which were more concentrated at the beginning and end of the intercomparison period. The well-mixed region of the marine boundary layer extended upwards to about 1.2 km (Figure 1).

[21] The first intercomparison flight (Flight 18 for the P3B and RF01 for the C130), unfortunately, could not be used in this study due to the large lateral separation between the aircraft. It is desirable to have the aircraft as close as possible, with nominal separations of less than 200 m in the horizontal and 10 m in the vertical to minimize differences [*Nicholls et al.*, 1983]. Unfortunately, the aircraft did not maintain the required vertical separation over time periods long enough to properly sample the MBL so the first intercomparison is not included in this analysis. Aircraft separations during the second intercomparison flight were close enough on three legs to allow useful intercomparisons to be made.

4. Results

[22] Three flight legs of P3B Flight 19 met our spatial and temporal separation criteria for intercomparing the two aircraft air-motion systems. They are summarized in Table 2 and consist of two legs at 152 m and one at 610 m altitude. These three legs, flown within the lower half of the MBL, are at different headings and angles to the prevailing wind direction. The horizontal separations,

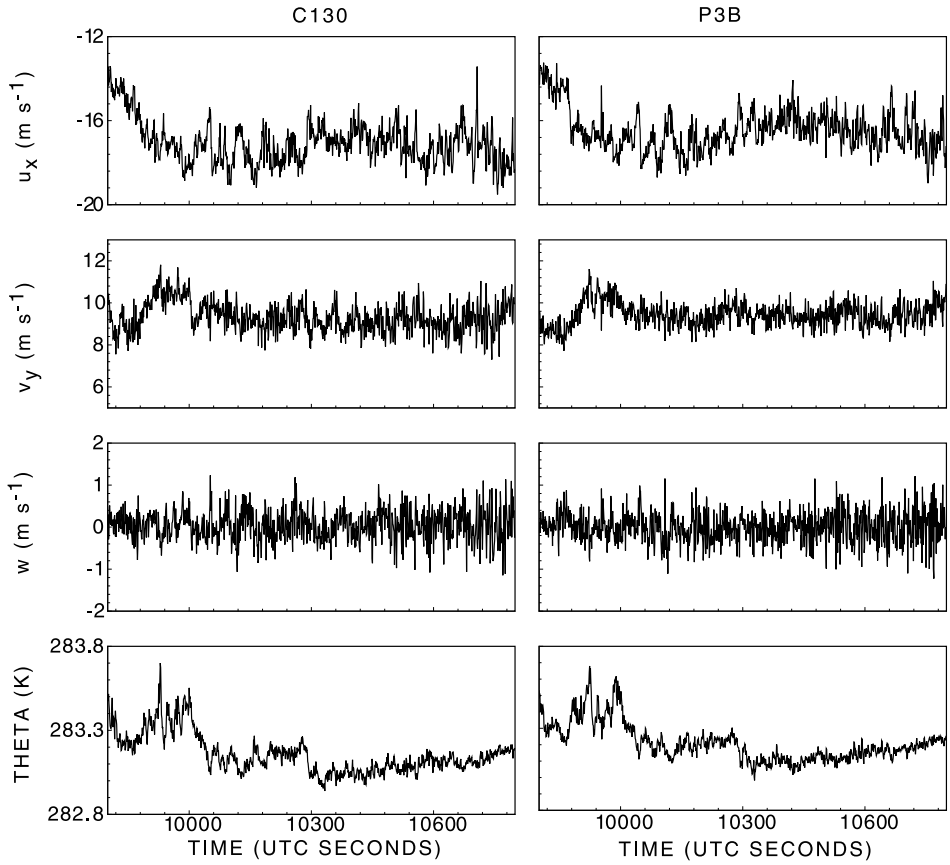

Figure 2. Time series plots of the air-motion measurements from the P3B and C130 from P3B Flight 19 (152 m segment).

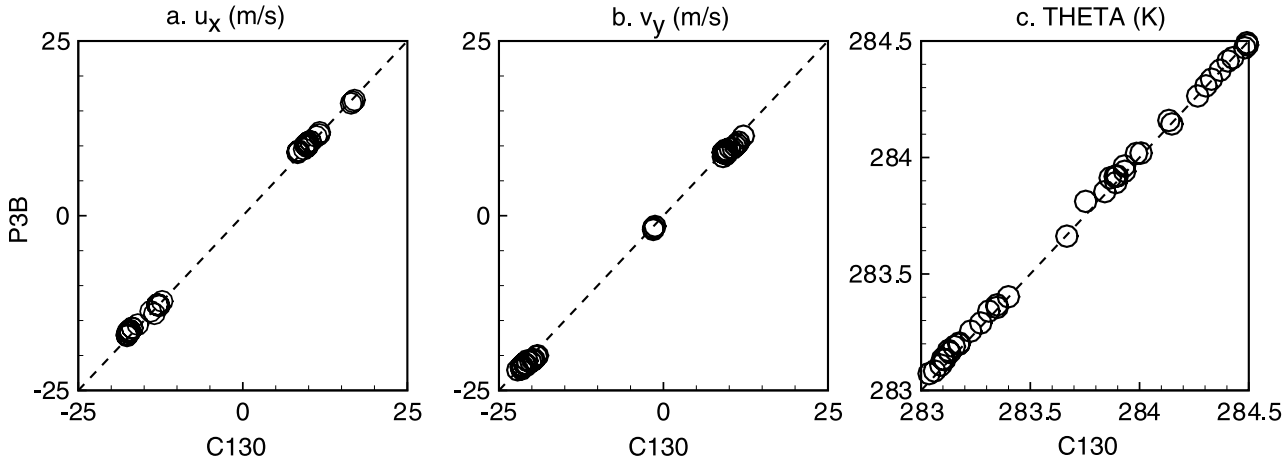

Figure 3. Scatter plots of the means of the horizontal winds (a–b) and potential temperature (c).

both longitudinal and lateral, were less than 200 m, as was determined from the INS and GPS data. The vertical separation was generally less than 10 m as determined from radar altimeter data.

[23] High-frequency data recorded on each flight leg were further separated into 4096-pt segments for linear detrending to remove unresolvable low-frequency components associated with mesoscale dynamic features. At a nominal true air speed of 100 m s^{-1} and a sampling rate of 25 s^{-1}, these 4096-point data blocks represent 16.4 km of flight path. The detrending primarily affects the variances. Finally, the segments were overlapped by 50% to better sample all flux carrying frequencies and reduce the error in statistical averages [*Bendat and Piersol*, 1993]. The spectra and cospectra were smoothed for presentation and analysis using block averaging with ten frequency intervals per decade. The

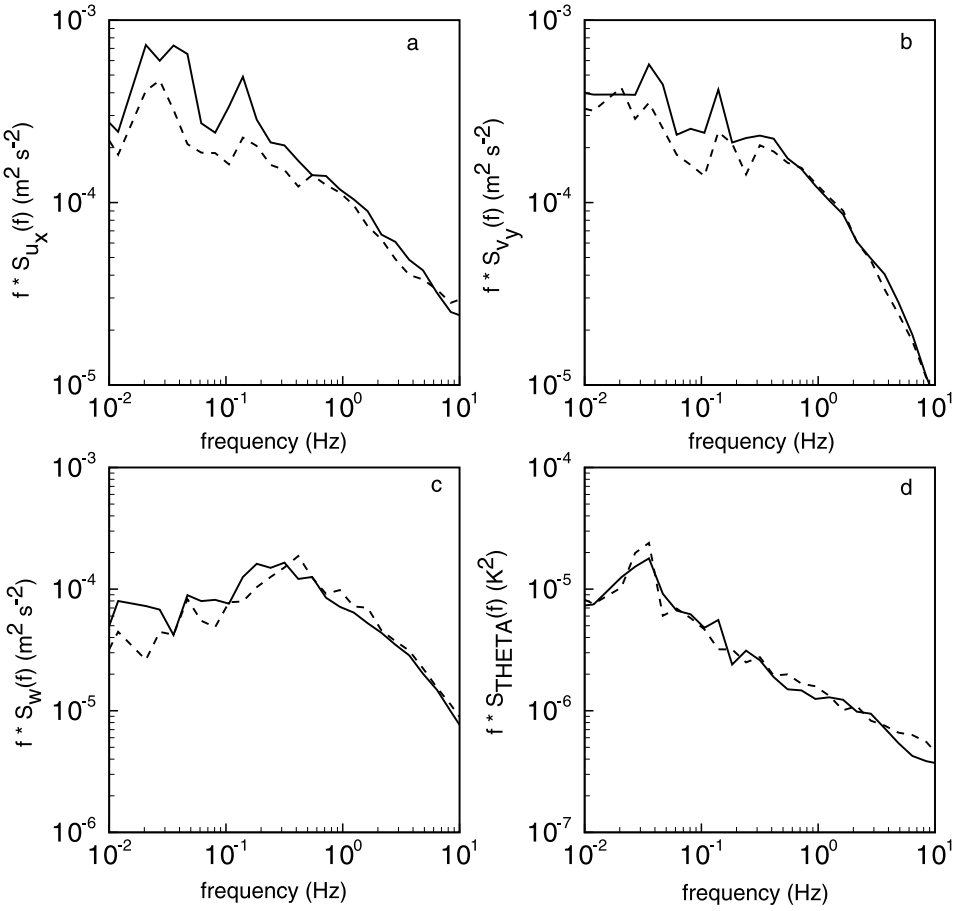

Figure 4. Power spectra of the horizontal winds (a–b), vertical winds (c), and potential temperature for the NCAR EC-130Q (solid line) and the NASA P3-B (dashed line).

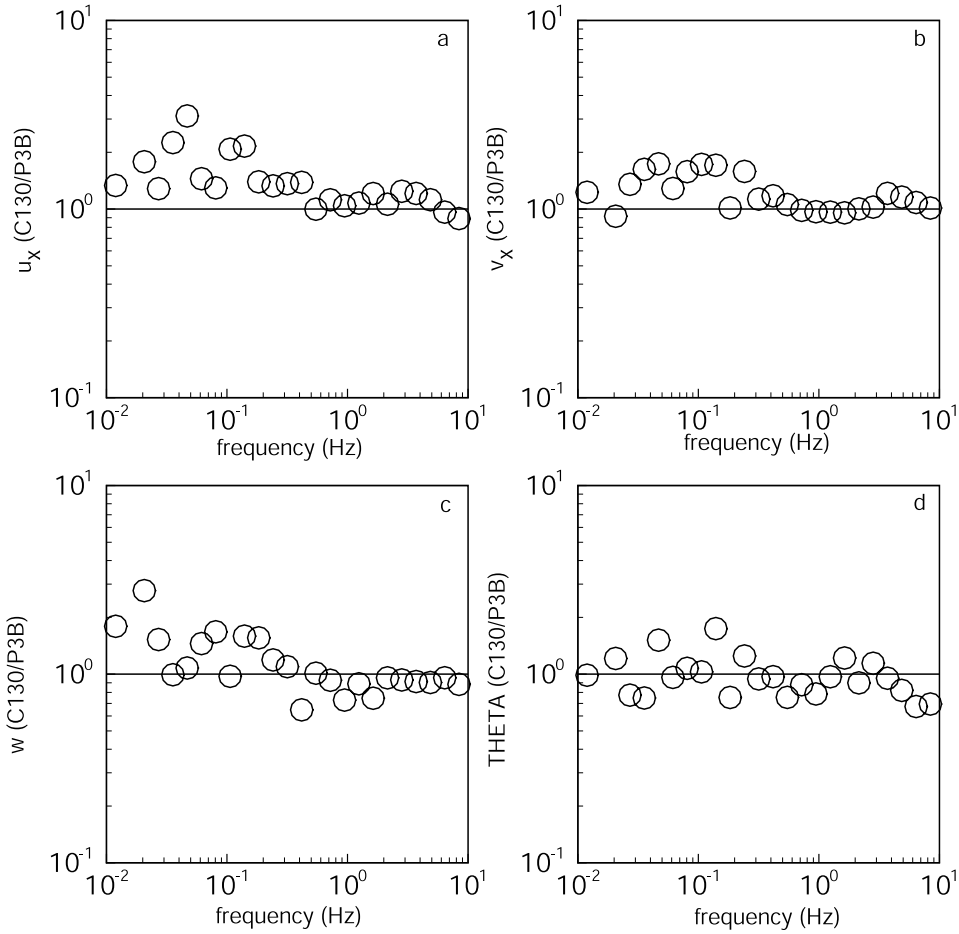

Figure 5. Power spectral ratios of the horizontal winds (a–b), vertical winds (c), and potential temperature (d) for the NCAR EC-130Q (solid line) and the NASA P3-B.

smoothing algorithm was modeled after *Kaimal and Gaynor* [1983].

[24] Our analysis focused upon examining differences in the means, variances, and covariances of the wind and potential temperature (theta) data produced by the two aircraft systems. Because the P3B Lyman-Alpha did not function during Flight 19, it is not possible to compare the humidity related parameters. The winds are presented in a coordinate system defined by the true heading of the aircraft, with vertical defined as the local earth vertical. Thus the horizontal components are the longitudinal (u_x) and the lateral (v_y) components with respect to the aircraft, as opposed to an Earth-based coordinate system of u (East) and v (North). This type of reference system allows the individual systems on each aircraft to be compared independently since the air motion sensors measure with respect to the longitudinal axis of the aircraft [*Lenschow et al.*, 1991]. A drawback to this method is that it could conceivably decrease the correlation between horizontal components if the headings of the aircraft are not the same. This effect is neglected in this analysis, a method similarly used by *Lenschow et al.* [1991].

4.1. Time Series

[25] We first look at means and trends of the air motion measurements. Significant problems or errors in sensor performance or measuring techniques can become immediately apparent when looking at time series. The time series recorded during the two intercomparison flights exhibit excellent agreement, even with the aforementioned spatial differences in the aircraft positions. An example of the mean values for the three-dimensional winds, and potential temperature is shown in Figure 2 for a 152 m leg of Flight 19. This is a 1000-s segment of the leg flown in the PBL shortly after the beginning of the intercomparison period about 11:45 AM local time (Japan Standard Time). The mean values show strong agreement, especially for the lower frequency components of the winds and potential temperature.

[26] Scatter plots of the mean values of several air motion parameters recorded aboard the two aircraft are shown in Figure 3. Each point represents averages computed from 4096-point segments. Each scatter plot shows consistent results between the air motion systems, with slopes and intercepts of approximately one and zero, respectively.

[27] An added level of confidence in the mean air motion measurements was gained by the system's responses during aircraft maneuvers (nonstraight and level flight). Although no predetermined maneuvers such as pitching or crabbing were performed to compare responses, ramp and spiral ascents/descents were made for tropospheric profiling and to acquire measurements for satellite validation purposes.

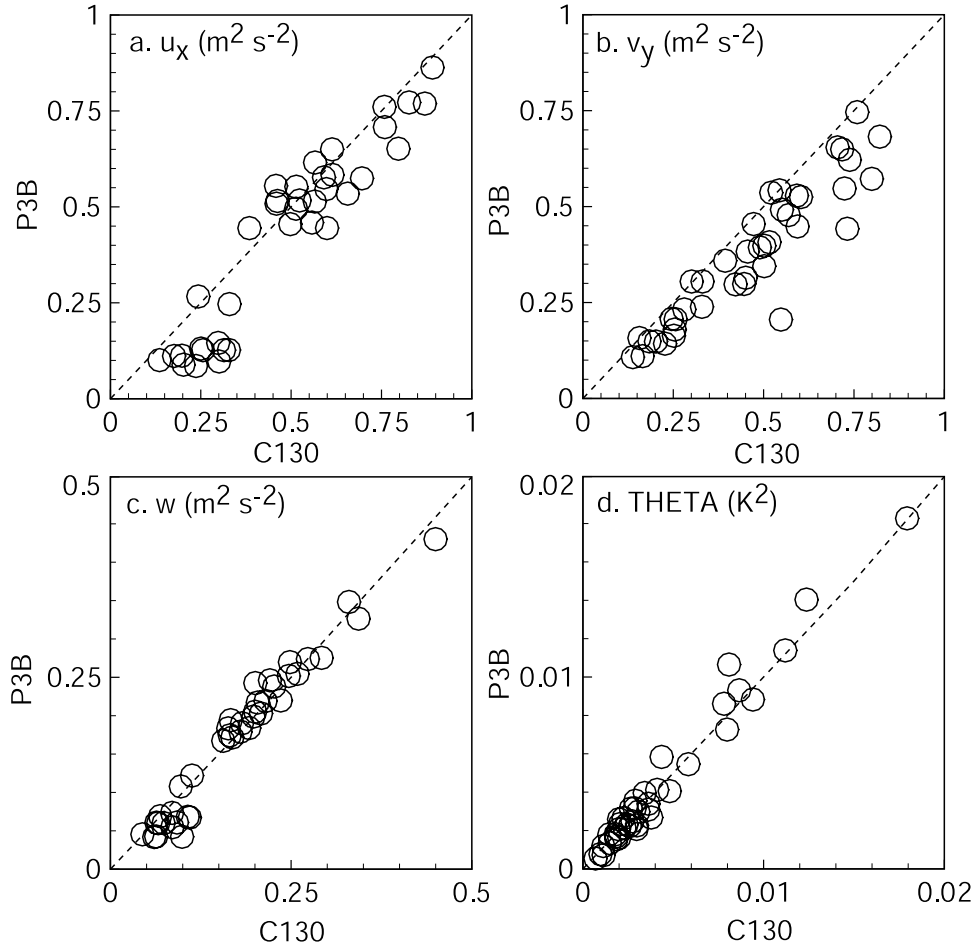

Figure 6. Comparison of variances. (a) Longitudinal Wind (u_x); (b) Lateral Wind (v_y); (c) Vertical Wind (w); (d) Potential Temperature. The solid line shows perfect 1:1 agreement.

Examples of the resulting winds and temperature can be seen in Figure 1, which displays vertical soundings from the second intercomparison flight made during a spiral descent into the MBL that show measurements from neither air motion system is influenced by the aircraft maneuvers. Such observations are useful, not for looking at absolute differences in the data between the two aircraft, but to ensure that aircraft motion is completely decoupled from the air motion measurements that appropriate calibration coefficients are used for calculating the lateral and longitudinal wind components.

[28] Inertial navigation systems are known to produce errors that limit the accuracy of horizontal wind calculations. Alignment and accelerometer errors result in signal drift and Schuler oscillations due to the integrating of accelerations to produce velocity and position measurements. GPS data is a perfect compliment to the INS data, since it does not suffer from the Schuler oscillation or positional drift. Thus the high frequency (25 Hz) INS data can be blended with low frequency (1 Hz) GPS information to produce more accurate aircraft platform velocities which in turn result in more precise horizontal wind measurements. At the time of TRACE-P, the P3B TAMMS did not record GPS positional data and thus INS/GPS coupling cannot be used to remove the INS errors in the horizontal wind measurements. An examination of the corrected versus uncorrected aircraft velocities from the C130 showed that the aircraft velocities were affected by about ±1 m s^{-1} for the mean longitudinal aircraft velocity and about ±0.7 m s^{-1} for the mean lateral aircraft velocity.

4.2. Variances

[29] Fourier power spectra and cospectra of air motion parameters are typically examined to determine the fidelity of signals, calculate fluxes, delineate atmospheric dynamical features, and isolate noise sources. The Fourier spectrum shows the signal response as a function of frequency while the cospectrum shows the relationship between two signals, vertical velocity and humidity, for example. The integral of the Fourier spectra is the variance of the signal, and the integral of the cospectra is the covariance.

[30] The power spectra for the intercomparison run at 610 m on P3B Flight 19 are shown in Figure 4. Since the Lyman-Alpha source was not functional on Flight 19, only the winds and the potential temperature can be compared. Each power spectral plot is an average of 17, 4096-pt segments, except for the potential temperature which is only 15 segments. The last two segments of this time series were discounted because greater variance and structure was seen in the P3B data than in the C130 signals near the end of the leg at a time when the aircraft reached their maximum spatial separation. It was decided that including these data biased

the potential temperature spectral comparison. Removing the last two segments reduced the length of the leg by about 90 s with the overlap or about 5% of the data for that leg.

[31] The horizontal wind components agree well in the inertial subrange, at frequencies greater than 1–2 Hz. This shows that the errors in true airspeed (longitudinal wind) and sideslip angle (lateral wind) have been accounted for. The horizontal winds exhibit the correct slope in the inertial subrange (−2/3 for the plots in Figure 4). The primary differences in the spectra arise at frequencies less than 1 Hz. Clearly, Figure 4 shows that the C130 has more variance in the horizontal winds in this region. Except for a difference in magnitude, the spectral shapes are very similar.

[32] An examination of the track angles from the two aircraft shows that the P3B was the lead aircraft, under autopilot control, while the C130 flew as the pacer aircraft, under manual control. The power spectra of the inputs to the horizontal winds (not included) indicated that the power spectra of the C130 signals had peaks in the low-frequency region of air speed and sideslip (affecting the spectra of the calculated horizontal winds) that coincide with the differences in the spectra of the two aircraft. Ideally, all aircraft motion is accounted for in the wind equations via calibrations. However, since the intercomparison was flown by the C130 in less than optimum conditions, the results could have been affected. The longitudinal wind (Figure 4a), which is dominated in the high-frequency region by the response of the true air speed falls off at the expected −2/3 slope. However, the lateral horizontal wind, strongly influenced in the inertial subrange by the response of the sideslip angle from the radome falls off steeper than a −2/3 slope at frequencies greater than 4 Hz. This feature is observed in the lateral wind for both aircraft. This is due to low-pass filter in the data-acquisition systems on each aircraft. The similar fall off is observed at frequencies greater than 4 Hz for the horizontal winds due to the radome angle of attack measurements.

[33] The power spectra of the vertical wind (Figure 4c) demonstrates that the C130 has more variance in the low-frequency portion of the spectra, while the high-frequency regions match very closely throughout the inertial subrange. The low-frequency difference is again, attributed to the aircraft motion induced by pilot corrections to maintain flight formation with the P3B.

[34] Figure 4d displays power spectra of potential temperature. The C130 spectrum shows −2/3 slope in the inertial subrange out to about 8 Hz, when it rolls off. The P3B spectrum matches that of the C130 throughout the entire frequency range, however both spectra exhibit slopes of >−2/3 (i.e., less steep) at higher frequencies, possibly due to white noise background on the temperature signals.

[35] Another way to compare the frequency response of the two aircraft is to examine the spectral ratios of turbulence parameters. Deviations of these ratios from unity can reveal limited sensor response, faulty processing algorithms, or instrument malfunctions. Spectral ratios for winds and potential temperature are presented in Figure 5 and reinforce the results shown in Figure 4. Whereas most of the ratios are between 0.8 and 1.2 in the high-frequency range, some show significant deviations in the low-frequency spectral region. The limited temporal response of the C130's vertical wind component is responsible for the roll-off in the w ratio at high frequencies seen in Figure 5c. The ratios are consistent with the results presented by *Nicholls et al.* [1983] and *Lenschow et al.* [1991].

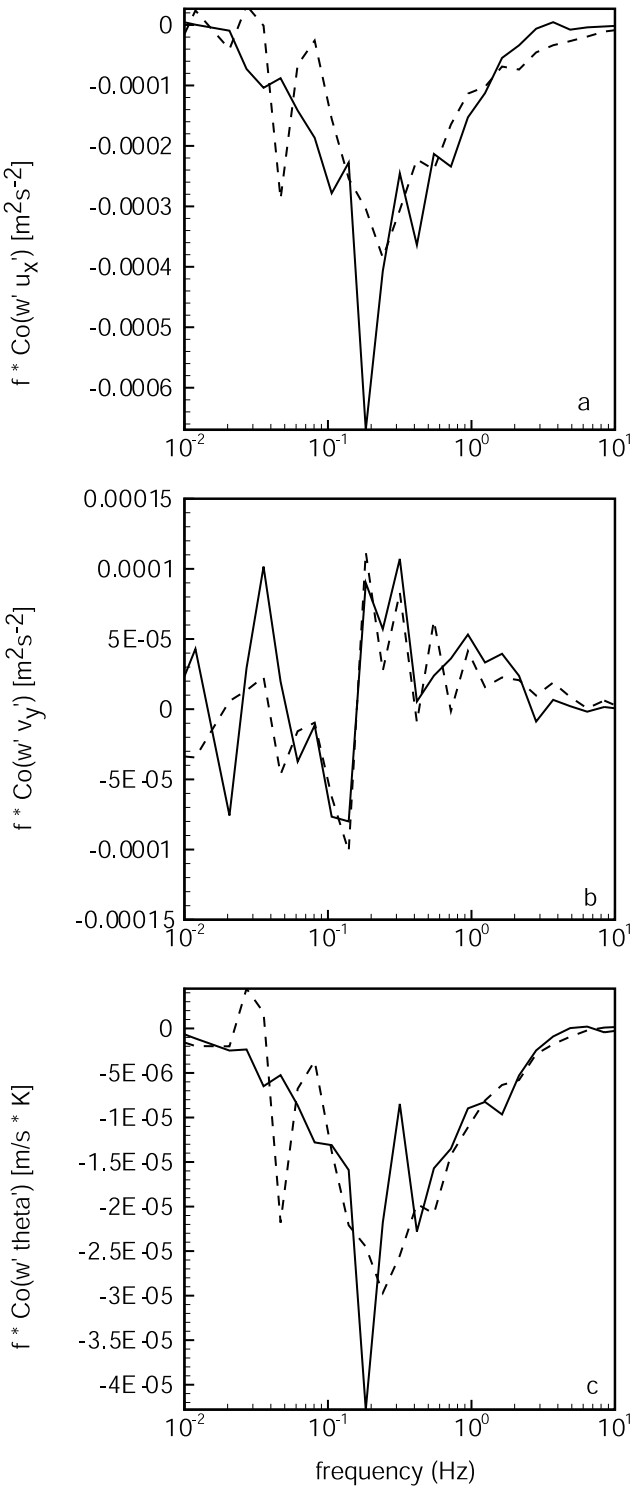

Figure 7. Cospectrum of the vertical winds and (a) longitudinal horizontal wind, (b) lateral horizontal wind, and (c) potential temperature for P3-B Flight 19 (0216:00–0226:00 UTC). The solid line is the NCAR C-130 and the dashed line is the NASA P-3B.

[36] The integrated variance results of all the intercomparison segments are presented as scatter plots in Figure 6.

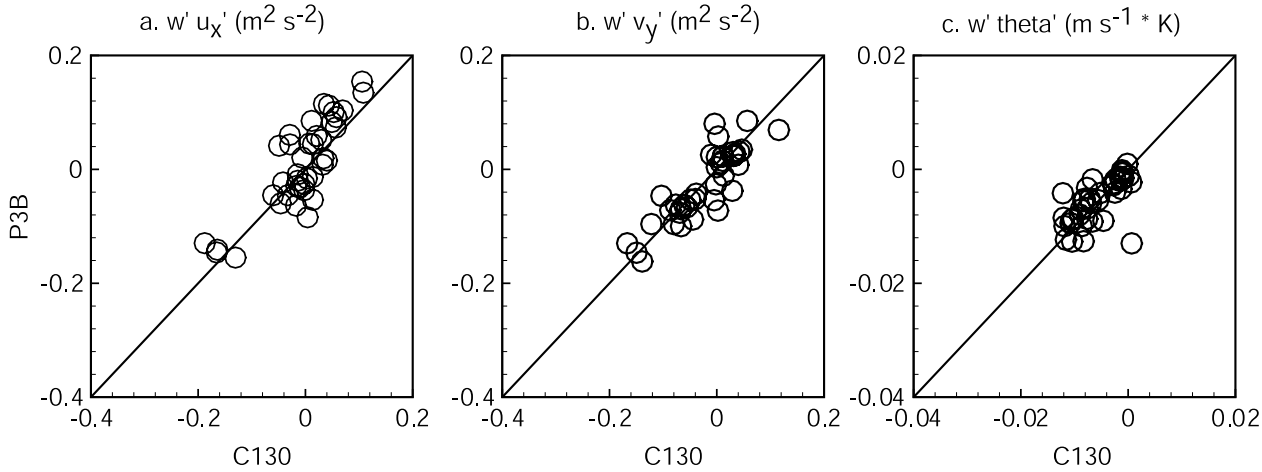

Figure 8. Covariance comparison of the vertical winds with the horizontal winds (a–b) and potential temperature (c) for the NCAR EC-130Q (x-axis) and the NASA P3-B (y-axis). The solid line shows perfect 1:1 agreement. Each point represents 4096 points of data (about 164 s).

Ideally, the results would all fall along the 1:1 line. The horizontal winds exhibit the greatest scatter because of the additional variance induced into the C130 wind signals by the repeated heading, altitude, and airspeed corrections it made to maintain pace with the P3B This creates a departure in the variances from the 1:1 line as the variance of the horizontal winds increase. The vertical winds and potential temperature have the least amount of scatter since the aircraft motion is not as important in the variance calculations of these parameters. Even with the scatter, the variances appear very consistent.

4.3. Covariances

[37] The integral of the covariance of the vertical velocity with another measurement such as potential temperature is the turbulent flux. By comparing the cospectrum of the two air motion systems for a given pair of measurements, wavelength regions where there is a disagreement become apparent. The cospectrum can show whether the response from an aircraft is limited at low frequencies due to signal resolution and/or instrument drift or high frequencies because of instrument signal frequency response [*MacPherson et al.*, 1992] or, by examining the relative amplitudes of the spectra, if the two signals are properly phased with one another.

[38] Using the eddy correlation method, three fluxes were computed for this instrument intercomparison: the horizontal momentum fluxes (longitudinal and lateral) and the sensible heat flux. Again, the data was linearly detrended but not high-pass filtered to compute the fluxes. Figure 7 shows the cospectra for one of the 152 m legs on P3B Flight 19. The greatest difference in cospectra from Figure 7 is a spike in the $w'u'_x$ and w′theta′ cospectra, where there is a large downward flux in the C130 measurements at 0.2 Hz. A similar spike is observed in the $w'v'_y$ cospectra by the C130, but there it is also seen in the P3B cospectra. The terms with the primes are the turbulent fluctuations of the variable (e.g., $w = \overline{w} + w'$ and $\overline{w}' = 0$). The momentum fluxes are most subject to error due to the complex corrections required in calculating the three-dimension wind [*Dobosy et al.*, 1997]. In addition, generally weak correlation is observed between the horizontal and vertical winds which add to the random error of the fluxes [*Lenschow and Stankov*, 1986].

[39] The peaks in the cospectrum occur at about 0.2 Hz, which is about a wavelength of ~500 m. The fluxes also taper off to zero at the high-frequency and low-frequency ends of the cospectrum. This indicates that the sample rate and time series length are sufficient to account for all the flux carrying wavelengths.

[40] The integrated fluxes are presented in Figure 8 for all the 4096-pt segments as scatter plots. The best results are, as anticipated, with the sensible heat flux, which tends to fall upon the 1:1 line (Figure 8c). The lateral momentum flux (Figure 8b) is the better of the two horizontal momentum fluxes, while the longitudinal momentum flux has a group of points where the P3B data produces overestimates of the momentum flux (or the C130 data gives underestimates). The greater variability observed in the momentum flux is mostly due to the weak correlation observed between horizontal and vertical wind components, this makes any small error in computing the winds (e.g., phase angle) amplified. The platform motion contamination of the mean horizontal wind components should not be greatly impact the momentum fluxes because the vertical wind component used to calculate the covariances is essentially independent of lateral and longitudinal accelerations.

5. Conclusions

[41] An intercomparison between the air motion systems of the NASA P3B and the NCAR C130 was performed in the spring of 2001 over the Sea of Japan. Both aircraft were four-engine turboprops with radome flush mount pressure measuring systems. The time series, variances, and covariances were analyzed and compared. Using the criteria of having a nominal aircraft separation distance of <200 m horizontally and 10 m vertically, legs at three altitudes from one of the two intercomparison flights were selected for detailed analysis.

[42] The results of the intercomparison show good agreement for the air motion systems. The greatest differences

were found in the horizontal wind components. Because of instrument limitations, absolute accuracies in the horizontal winds on the P3-B were reduced by an inability to correct for INS drift using GPS coupling. The time series results showed that the mean aircraft measurements of the winds and potential temperature were good for time periods of at least 2–3 min. The regression slopes for the mean winds and potential temperature were nearly unity. The variances and spectra for horizontal winds exhibited differences at low frequencies that were attributed INS drift on the P3B and contamination by platform motion on the C130 as it attempted to follow the P3B in formation. Spectra of vertical winds suggest that the C130 system has a slightly lower temporal response that used on the P3B. Variances of potential temperature recorded aboard the aircraft are in good agreement and cospectral result indicate that the calculated meteorological fluxes are also comparable and well within the expected levels of uncertainty for both aircraft systems.

[43] Overall, output from the air motion systems on the aircraft agree remarkably well considering the potential sources of error. Although the aircraft were flown within 200 m of each other horizontally and 10 m vertically, the chosen air mass exhibited considerable horizontal inhomogeneities. In addition, radome based systems rely on two types of calibrations to produce accurate winds. The first is calibrating the static pressure deficit and the second is determining the coefficients for the angles of sideslip and attack. Although the calibration methods are similar between the two aircraft, small differences can change the calculated winds significantly, as they are very sensitive to any error in calibrations. Finally, as mentioned above, the P3B currently does not employ a method to correct the INS drift with GPS position updates. This can result in errors in the winds on the order of 1 m s^{-1}. A suitable GPS system has subsequently been installed aboard the P3B and its output will be blended with that of the INS to produce improved long-term measurements of platform position and velocity and hence horizontal winds.

[44] Even with the above potential problems, the end results of this intercomparison are very encouraging given the number of high-precision, fast-response measurements required to calculate the winds. No systematic errors were discovered in either system that would negatively impact their ability to be used for quantitative, eddy-correlation flux determinations. The TAMMS group is presently engaged in upgrades to its air motion capabilities, such as implementing the GPS coupling algorithms, reducing hardware weight for payload concerns, and developing/acquiring a new fast response water vapor sensor.

[45] **Acknowledgments.** The authors would like to thank the science teams from both the TRACE-P and ACE-ASIA field missions. We thank both the WFF P-3B and the NCAR EC-130Q ground and flight crews for their excellent support. This research was supported by the NASA Global Tropospheric Chemistry Program. The National Center for Atmospheric Research is sponsored by the National Science Foundation.

References

Barrick, J. D. W., J. A. Ritter, C. E. Watson, M. W. Wynkoop, J. K. Quinn, and D. R. Norfolk, Calibration of NASA turbulent air motion measurement system, *NASA Tech. Pap. TP-310*, NASA, Washington, D. C., 1996.

Bendat, J. S., and A. G. Piersol, *Engineering Applications of Correlation and Spectral Analysis*, John Wiley, Hoboken, N. J., 1993.

Blanchard, R. L., A new algorithm for computing inertial altitude and vertical velocity, *IEEE Trans. Aerosp. Electron. Syst.*, *AES-7*, 1143–1146, 1971.

Brown, E. N., C. A. Friehe, and D. H. Lenschow, The use of pressure fluctuations on the nose of an aircraft for measuring air motion, *J. Clim. Appl. Meteorol.*, *122*, 171–180, 1983.

Considine, G. D., B. E. Anderson, J. D. W. Barrick, and D. H. Lenschow, Characterization of turbulent transport in the marine boundary layer during flight 7 of PEM-TROPICS A, *J. Geophys. Res.*, *104*(D5), 5855–5863, 1999.

Deleo, R. V., and F. D. Werner, Temperature sensing from aircraft with immersion sensors, paper presented at Fall Instrument-Automation Conference, Instrum. Soc. Of Am., New York, 26–30 September 1960.

Dobosy, R. J., T. L. Crawford, J. I. MacPherson, R. L. Desjardins, R. D. Kelly, S. P. Oncley, and D. H. Lenschow, Intercomparison among four flux aircraft at BOREAS in 1994, *J. Geophys. Res.*, *102*(D24), 29,101–29,111, 1997.

Jacob, D. J., J. H. Crawford, M. M. Kleb, V. E. Connors, R. J. Bendura, J. L. Raper Jr., G. W. Sachse, J. C. Grille, and L. Emmons, The Transport and Chemical Evolution over the Pacific (TRACE-P) mission: Design, execution, and first results, *J. Geophys. Res.*, *108*(D20), 8781, doi:10.1029/2002JD003276, in press, 2003.

Kaimal, J. C., and J. E. Gaynor, The Boulder Atmospheric Observatory, *J. Clim. Appl. Meteorol.*, *22*, 863–880, 1983.

Khelif, D., S. P. Burns, and C. A. Friehe, Improved wind measurements on research aircraft, *J. Atmo. Oceanic Tech.*, *16*, 860–872, 1999.

Larson, T. J., S. G. Flechner, and P. M. Siemers, Wind tunnel investigation of an all flush orifice air data system for large subsonic aircraft, *NASA Tech. Pap. TP-1642*, NASA, Washington, D. C., 1980.

Lemone, M. A., and W. T. Pennell, A comparison of turbulence measurements from aircraft, *J. Appl. Meteorol.*, *19*, 1420–1437, 1981.

Lenschow, D. H., (Ed.), *Probing the Atmospheric Boundary Layer*, Am. Meteorol. Soc., Boston, Mass., 1986.

Lenschow, D. H., and P. Spyers-Duran, Measurement techniques: Air motion sensing, *NCAR Research Aviation Facility Bull. 23*, 36 pp., Natl. Cent. for Atmos. Res., Boulder, Colo., 1989. (Available from NCAR, P. O. Box 3000, Boulder, CO 80307, USA)

Lenschow, D. H., and B. B. Stankov, Length scales in the convective boundary layer, *J. Atmos. Sci.*, *43*, 1198–1209, 1986.

Lenschow, D. H., E. R. Miller, and R. B. Friesen, A three-aircraft intercomparison of two types of air motion measurement systems, *J. Atmos. Oceanic Tech.*, *8*, 41–50, 1991.

MacPherson, J. I., R. L. Grossman, and R. D. Kelly, Intercomparison results from FIFE aircraft, *J. Geophys. Res.*, *97*(D17), 18,499–18,514, 1992.

Nicholls, S., W. Shaw, and T. Hauf, An intercomparison of aircraft turbulence measurements made during JASIN, *J. Clim. Appl. Meteorol.*, *22*, 1637–1648, 1983.

Ritter, J. A., D. H. Lenschow, J. D. W. Barrick, G. L. Gregory, G. W. Sachse, G. W. Hill, and M. A. Woerner, Airborne flux measurements and budget estimates of trace species over the Amazon Basin during the GTE/ABLE-2B expedition, *J. Geophys. Res.*, *95*(D10), 16,875–16,886, 1990.

Ritter, J. A., J. D. W. Barrick, G. W. Sachse, G. L. Gregory, C. E. Watson, M. A. Woerner, and J. E. Collins, Airborne flux measurements of trace species in an Artic boundary layer, *J. Geophys. Res.*, *97*(D15), 16,601–16,625, 1992.

Ritter, J. A., J. D. W. Barrick, C. E. Watson, G. W. Sachse, G. L. Gregory, B. E. Anderson, M. A. Woerner, and J. E. Collins, Airborne boundary layer flux measurements of trace species over Canadian boreal forest and northern wetlands regions, *J. Geophys. Res.*, *99*(D1), 1671–1685, 1994.

Schmitt, K. F., C. A. Friehe, and C. H. Gibson, Humidity sensitivity of atmospheric temperature sensors by salt contamination, *J. Phys. Oceanogr.*, *8*, 151–161, 1978.

B. E. Anderson, J. D. W. Barrick, and K. L. Thornhill, NASA Langley Research Center, Mail Stop 483, Hampton, VA 23681, USA. (b.e.anderson@larc.nasa.gov; j.d.barrick@larc.nasa.gov; k.l.thornhill@larc.nasa.gov)

D. R. Bagwell, NASA Langley Research Center, Mail Stop 156A, Hampton, VA 23681, USA. (d.r.bagwell@larc.nasa.gov)

R. Friesen and D. H. Lenschow, National Center for Atmospheric Research, P. O. Box 3000, Boulder, CO 80307-3000, USA. (dick@raf.atd.ucar.edu; lenschow@ncar.ucar.edu)